Photoluminescence induced by twinning interface in CdS nanocrystals

P. Q. Zhao,[1,2] S. J. Xiong,[2] X. L. Wu,[2,a)] and Paul K. Chu[3,a)]
[1]*Department of Applied Physics, Nanjing University of Technology, Nanjing 210009, People's Republic of China*
[2]*Department of Physics, Nanjing National Laboratory of Microstructures, Nanjing University, Nanjing 210093, People's Republic of China*
[3]*Department of Physics and Materials Science, City University of Hong Kong, Tat Chee Avenue, Kowloon, Hong Kong, China*

(Received 28 February 2012; accepted 12 April 2012; published online 25 April 2012)

The photoluminescence (PL) spectra acquired from CdS nanocrystals encapsulated with oleic acid synthesized by a two-phase approach exhibit two fine features, including a narrow peak arising from near-band edge emission and a broader one composed of two subpeaks at slightly lower energy. Solvent effects suggest that the surface defect states on the nanocrystals are not the origin of this broad PL band. High-resolution transmission electron microscopy examinations and density function theory calculation reveal that the broad low-energy PL band stems from twinning interfaces in the CdS nanocrystals. © *2012 American Institute of Physics*. [http://dx.doi.org/10.1063/1.4707388]

Group II-VI semiconductor nanocrystals (NCs) have been extensively studied due to adjustable emission in the visible range by varying the size and applications to light emitting and photovoltaic devices.[1–4] CdS, one of the common II-VI semiconductors, has a band gap of 2.42 eV at room temperature and is suitable for white-light emitting displays. Consequently, much work has been devoted to the preparation of high-quality CdS NCs.[5–7] In general, simple mixing of red-, green-, and blue emitting NCs can lead to possible undesirable changes in the chromaticity coordinates caused by different relative temporal stability of the components. Synthesis of semiconductor NCs with white-light emission such as ZnS:Pb, ZnS:Mn, and "magic-sized" CdSe have been reported,[8–10] but these materials systems rely on the surface state (sulfur vacancies, SVs) emission from the NCs. Recently, Nizamoglu *et al.*[11] reported that the use of a single type of such CdS NC luminophores was more advantageous than multiple combinations of NCs in solid-state lighting. However, the origin of the broad band photoluminescence (PL) from CdS NCs is still not well understood.

In this work, we investigate the PL properties of colloidal CdS NCs with different sizes synthesized by a simple two-phase approach. All the samples show a strong broad emission peak from 500 to 750 nm in addition to a relatively narrow near-band-edge luminescence peak at less than 500 nm. Spectral and structural analyses show that the broad emission band can be attributed to optical transition in the electronic states induced by twinning interfaces in the NCs. First-principle calculation also shows that the twin boundaries produce a large number of states within the gap and are responsible for the broad emission which is even stronger than that of the near band edge emission.

The CdS NCs were fabricated by a two-phase technique. Toluene and water were used as separate solvents for cadmium myristate (CdM_2) and thiourea serving as the cadmium source and sulfur source, respectively, and oleic acid (OA) was used as the ligand to stabilize the NCs. CdM_2 was prepared according to the procedures described earlier.[12] In the process, a mixture of CdM_2 (0.1134 g, 0.2 mmol), oleic acid (1 ml), and toluene (10 ml) was loaded into the Teflon liner of a 30-ml stainless steel autoclave and then heated at 90–100 °C to produce an optically clear solution. Afterwards, the autoclave was cooled to room temperature naturally, and an aqueous solution of thiourea (10 ml, 0.0304 g, 0.4 mmol) was added to the organic solution to form the two-phase system. The Teflon liner containing the mixture was then sealed in the stainless steel autoclave and maintained at 180 °C for 1 h. In the reactions adopted by the seeding-growth technique, three samples (a, b, and c) were synthesized orderly at slightly different temperatures.[13] The CdS NC colloidal solution was precipitated with methanol and isolated by centrifugation. The purified CdS NCs were dispersed in toluene or another organic solvent for further measurements. These samples were characterized by high-resolution transmission electron microscopy (HR-TEM) (Tecnai G2 F30 S-TWIN), energy dispersive x-ray spectroscopy (EDS), and PL (Edinburgh: FLS-920). All the measurements were conducted at room temperature.

The HR-TEM image of the OA-capped CdS NCs (sample a) in Fig. 1(a) reveals that the NCs have a narrow size distribution and are mostly spherical in shape. Fig. 1(b) shows the histogram of the size distribution of the NCs with a mean diameter about 4.2 nm, and Fig. 1(c) displays the EDS spectrum of individual CdS NCs in which the Cu signal arises from the copper mesh. The calculation indicates that the Cd^{2+} content is higher than that of S^{2-}, indicating that the NCs are sulfur deficient.

Figs. 2(a)–2(c) depict the room-temperature PL spectra of as-prepared samples a, b, and c, respectively, excited by the 380 nm line of a Xe lamp. These spectra show two PL bands. The high-energy band has a relatively narrow full-width at half-maximum (FWHM) of ~48 nm. It can be concluded from its position that this PL band is dominated by

a)Authors to whom correspondence should be addressed. Electronic addresses: hkxlwu@nju.edu.cn and paul.chu@cityu.edu.hk.

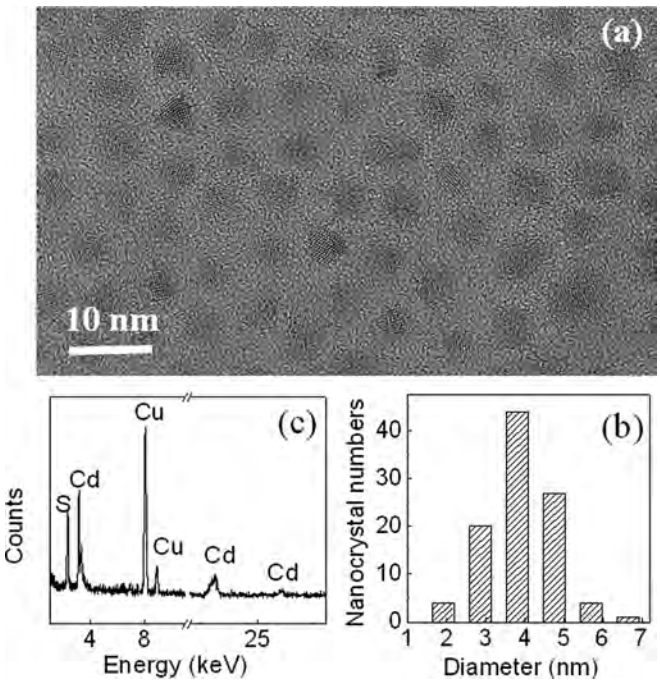

FIG. 1. (a) TEM image of the OA-capped CdS NCs for sample a. (b) Size distribution histogram. (c) EDS spectrum.

near-band-edge emission and arises from particles with the most probable diameter. The NC diameter, L, can be calculated by substituting E with 2.77 eV (448 nm for sample a), 2.68 eV (463 nm for sample b), and 2.60 eV (477 nm for sample c), respectively, based on the effective mass approximation of quantum size effect as shown in the following:[14]

$$E(r) = E_g + \pi^2 \left(\frac{a_B^*}{r}\right)^2 R_y^* - 3.572 \frac{a_B^*}{r} R_y^* - 0.248 R_y^*,$$

where $r = L/2$ and $E_g, R_y^*,$ and a_B^* are the bandgap energy (2.42 eV), exciton binding energy (0.028 eV), and exciton Bohr radius (2.8 nm), respectively. The estimated sizes are L = 4.3, 5.0, and 5.3 nm for samples a, b, and c, respectively,

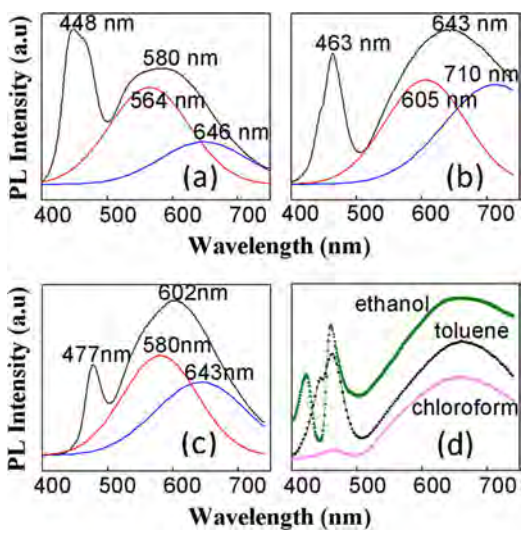

FIG. 2. Room-temperature PL spectra of the OA-capped CdS NCs in toluene in (a), (b), and (c) for three samples a, b, and c, respectively. (d) PL spectra of the OA-capped CdS NCs (sample b) dispersed in ethanol, toluene, and chloroform.

and almost the same as those calculated from the TEM images. This result further confirms the band edge recombination mechanism of the high-energy PL band. The second PL band is strong, broad, and asymmetrical in the range of 500–730 nm usually attributed to recombination of trapped charge carriers at surface defects due to either SVs or cadmium vacancies depending on the availability of cations or anions.[15–17] Since EDS shows that the content of Cd^{2+} content is higher than that of S^{2-}, the possibility of cadmium vacancies can be ruled out.

To investigate the roles of SVs, the second PL band with an asymmetrical emission is Gaussian deconvoluted into two subbands as shown in Fig. 2. The two sub bands suggest that two different locations of SVs in the CdS NCs, on the surface and inside the NCs. To rule out the influence of the surface defect states (including surface SVs), we examine the PL spectra of the CdS NCs [for sample b in Fig. 2(d)] dispersed in ethanol, toluene, and chloroform, respectively. Fig. 2(d) shows that the intensity of the first PL band from band edge recombination is obviously altered by the solvents,[18] but the second PL band arising from trapped states is basically unaffected. Hence, it can be inferred that the surface defect states are not the source of the broad PL band. Careful comparison of the two subbands in Fig. 2 discloses that their positions are different in the three samples and there is no NC size dependence. We have recently investigated that the depth dependence of the oxygen-vacancy-induced defects in ultrathin alumina nanoparticles and found that the energy of the oxygen-vacancy level increases with depth.[19] This indicates that the oxygen vacancy level has a dependence on the NC size. The larger the NC, the deeper is the mean depth of the oxygen-vacancy distribution and the higher the oxygen-vacancy level. A similar phenomenon is expected from SVs in CdS NCs. That is, sample c should have a higher SV level than samples a and b. However, this is not consistent with our experimental results in Fig. 2. Hence, the internal SVs also do not contribute to the low-energy broad PL band.

The HR-TEM images are further analyzed to fathom the mechanism. The CdS NCs contain many twinning NCs which are usually observed in grains with diameters smaller than 20 nm. A grain size effect is thus possible for the formation. Fig. 3 shows several representative magnified twin NCs. Twinning occurs along the {100} plane of the hexagonal wurtzite and {111} plane of cubic zinc blende in CdS NCs, and the twinning boundaries are clearly marked with white lines. The formation mechanism is usually considered to be due to partial dislocations at the grain boundaries, namely, dislocation mechanism in NC materials.[20] Hence, it is reasonable that the two low-energy PL subbands originate from optical transitions in the defect electronic states induced by twin interfaces. The PL spectra acquired from two samples annealed at 150 and 200 °C in the autoclave for 1 h indicate that the PL intensity of the 200 °C sample is reduced by a factor of 3 compared to that of the 150 °C one (data not shown). The experimental results provide more convincing evidence about the origin of the low-energy PL band.

To verify our hypothesis, first-principle calculation is performed on the electronic structure and optical properties

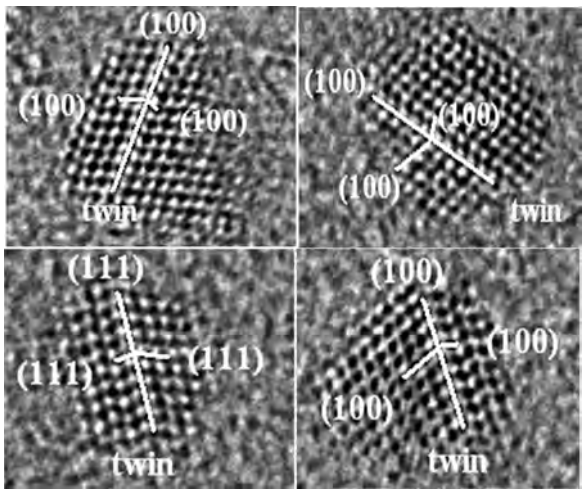

FIG. 3. Representative twinning structures in CdS NCs with the twinning plane along the {100} plane of hexagonal wurtzite and {111} plane of cubic zinc blende.

of the CdS surface with a twin interface perpendicular to the surface. The calculation is performed using the generalized gradient approximation (GGA) of the Perdew, Burke, and Ernzerholf (PBE) form[21] under package CASTEP (Ref. 22) adopting the plane-wave norm-conserving pseudopotential method.[23] We use a kinetic energy cutoff of 450 eV to represent the single-particle wave functions and adopt slabs to investigate the band structure and the optical properties of the {110} surface of CdS with the zinc blende structure. To form a periodic lattice, the slabs 1 nm thick are periodically stacked and separated with 1.2 nm thick vacuum slabs. The twin interface and the {111} plane form an angle α, and the interface is perpendicular to the surface of the slabs. The size of the supercell along the surface directions in the periodic structure is 0.8 nm $\times$ 0.8 nm. The geometry of the configuration is optimized using the Broyden-Fletcher-Goldfarb-Shanno (BFGS) minimizer in the CASTEP package with the following default convergence tolerances: 2×10^{-5} eV for energy change, 0.5 eV/nm for maximum force, and 0.02 nm for maximum displacement.[24] After geometric optimization, the band structure of electrons and optical properties are calculated using the CASTEP package.

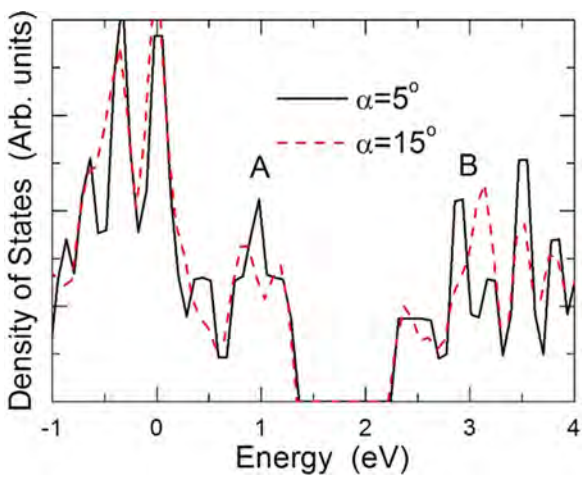

FIG. 4. Calculated density of states for the {110} surface of zinc blende CdS with twin boundaries perpendicular to the surface with α being the angle between the twin boundaries and the {111} plane.

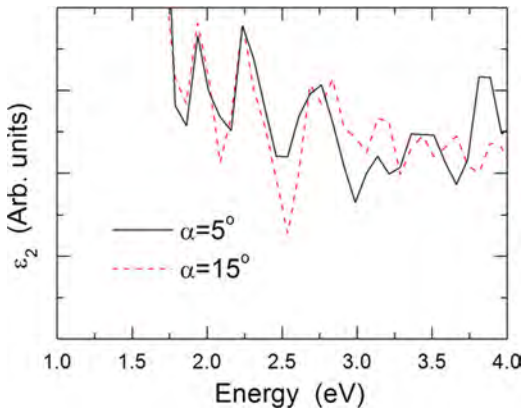

FIG. 5. Calculated imaginary part of dielectric function for samples for different values of α.

Fig. 4 plots the calculated density of states for samples with different angles α. By introducing the twin interface perpendicular to the surface, electronic states within the gap show some structures, as shown by the peaks marked with A in Fig. 4. These peaks are above the valence band top by about 0.5–1 eV, and so should be responsible for the broad and asymmetrical emission in 500–730 nm observed in our experiments. By increasing the angle between the twin interface and the {111} plane, the peak A may split into two peaks. On the other hand, although there is only one peak at A for the case of smaller α, peak B near the conduction band edge is split. This means that there are always two peaks in this energy range in the PL spectrum. For further confirmation, Fig. 5 plots the imaginary part of the dielectric function, ε_2. There are indeed two peaks in the range of 1.7 – 2.2 eV for both samples. Compared to the two peaks induced by twin boundaries, the peak near 2.8 eV arising from the near band edge emission is even weaker, as confirmed by the experimental results in Fig. 2. Here, we apply a scissors operator of 0.8 eV in CASTEP to compensate for the systematic underestimation of the band gap in GGA. The results show that splitting of peaks A or B does not depends on the NC size, but rather the angle between the twin interface and the {111} plane. This is the reason why the low-energy broad PL band has no orderly peak positions in our three samples a, b, and c.

In conclusion, the PL properties of CdS NCs with various twinning interfaces are studied. Microstructural and spectral analyses reveal that the high-energy blue PL band arises from the near band edge emission, but the low-energy broad band does not depend on SVs which are usually considered to exist in CdS NCs. Our DFT calculations clarify that the broad low-energy PL band stems from optical transition in the electronic states induced by the twinning interfaces in CdS NCs.

This work was jointly supported by National Basic Research Program of China (No. 2011CB922102), National Natural Science Foundation of China (No. 60976063), and PAPD. Partial support was from the Hong Kong Research Grants Council (RGC) General Research Funds (GRF) CityU 112510.

[1]M. Kuwata-Gonokami and K. Takeda, Opt. Mater. **9**, 12 (1998).
[2]P. O. Anikeeva, J. E. Halpert, M. G. Bawendi, and V. Bulovi, Nano Lett. **7**, 2196 (2007).

[3]A. P. Alivisato, Science **271**, 933 (1996).
[4]S. Coe, W. K. Woo, M. Bawendi, and V. Bulovic, Nature **420**, 800 (2002).
[5]C. B. Murray, D. J. Norris, and M. G. Bawendi, J. Am. Chem. Soc. **115**, 8706 (1993).
[6]J. Lee, V. C. Sundar, J. R. Heine, M. G. Bawendi, and K. E. Jensen, Adv. Mater. **12**, 1102 (2000).
[7]Z. A. Peng and X. G. Peng, J. Am. Chem. Soc. **123**, 183 (2001).
[8]A. A. Bol and A. Meijerink, Phys. Chem. Chem. Phys. **3**, 2105 (2001).
[9]H. Y. Lu, S. Y. Chu, and S. S. Tan, Jpn. J. Appl. Phys., Part I **1**, 5282 (2005).
[10]M. J. Bowers II, J. R. McBridge, and S. J. Rosenthal, J. Am. Chem. Soc. **127**, 15378 (2005).
[11]S. Nizamoglu, E. Mutlugun, O. Akyuz, N. K. Perkgoz, H. V. Demir, L. Liebscher, S. Sapra, N. Gaponik, and A. Eychmüller, New J. Phys. **10**, 023026 (2008).
[12]D. C. Pan, S. C. Jiang, L. J. An, and B. Z. Jiang, Adv. Mater. **16**, 982 (2004).
[13]Q. Wang, D. C. Pan, S. C. Jiang, X. L. Ji, L. J. An, and B. Z. Jiang, Chem.-Eur. J. **11**, 3843 (2005).
[14]Y. Kayanuma, Phys. Rev. B **38**, 9797 (1988).
[15]S. F. Wuister and A. Meijerink, J. Lumin. **105**, 35 (2003).
[16]H. M. Chen, X. F. Huang, L. Xu, J. Xu, K. J. Chen, and D. Feng, Superlattices Microstruct. **27**, 1 (2000).
[17]W. Chen, Y. Xu, Z. Lin, Z. Wang, and L. Lin, Solid State Commun. **105**, 129 (1998).
[18]U. Resch, A. Eychmüller, M. Haase, and H. Weller, Langmuir **8**, 2215 (1992).
[19]X. L. Wu, S. J. Xiong, J. H. Guo, L. L. Wang, C. Y. Hua, Y. Y. Hou, and P. K. Chu, J. Phys. Chem. C **116**, 2356 (2012).
[20]Y. M. Wang, A. M. Hodge, J. Biener, A. V. Hamza, D. E. Barnes, K. Liu, and T. G. Nieh, Appl. Phys. Lett. **86**, 101915 (2005).
[21]J. P. Perdew, K. Burke, and M. Ernzerhof, Phys. Rev. Lett. **77**, 3865 (1996).
[22]S. J. Clark, M. D. Segall, C. J. Pickard, P. J. Hasnip, M. J. Probert, K. Refson, and M. C. Payne, Z. Kristallogr. **220**, 567 (2005).
[23]D. R. Hamann, M. Schluter, and C. Chiang, Phys. Rev. Lett. **43**, 1494 (1979).
[24]B. G. Pfrommer, M. Cote, S. G. Louie, and M. L. Cohen, J. Comput. Phys. **131**, 233 (1997).